Raman Investigation of the Ionic Liquid *N*-Methyl-*N*-propylpyrrolidinium Bis(trifluoromethanesulfonyl)imide and Its Mixture with $LiN(SO_2CF_3)_2$

M. Castriota,[†] T. Caruso,[†] R. G. Agostino,[†] E. Cazzanelli,[†] W. A. Henderson,[‡] and S. Passerini*[,‡]

LiCryl−INFM (Liquid Crystal Regional Laboratory), c/o Department of Physics, University of Calabria, Via P. Bucci Cubo 31C, I-87036 Rende (CS), and ENEA (Italian Agency for New Technologies, Energy and the Environment), IDROCOMB, C.R. Casaccia, Via Anguillarese 301, 00060 Rome, Italy

Received: September 2, 2004; In Final Form: October 13, 2004

A preliminary Raman investigation of the ionic liquid *N*-methyl-*N*-propylpyrrolidinium bis(trifluoromethanesulfonyl)imide ($PYR_{13}TFSI$) and its 2/1 complex with the lithium salt $LiN(SO_2CF_3)_2$ is reported. The study was performed over a temperature range extending from −100 to +60 °C, i.e., with $PYR_{13}TFSI$ in the crystalline and melt states. For comparison purposes, the study was extended to $PYR_{13}I$, which is the precursor used in the synthesis of $PYR_{13}TFSI$.

Introduction

Room temperature ionic liquids (RTILs) are a rapidly expanding topic of research due to their favorable properties such as negligible volatility, high chemical, thermal, and electrochemical stability, high ionic conductivity, and, in some cases, hydrophobicity.[1−4] These properties make them very attractive candidates for use in electrolytes for electrochemical applications such as the electrodeposition of electropositive metals, light-emitting electrochemical cells, photoelectrochemical cells, electrochemical capacitors, fuel cells, and batteries.[5−14]

Very recently we have shown that the addition of *N*-methyl-*N*-propylpyrrolidinium bis(trifluoromethanesulfonyl)imide ($PYR_{13}TFSI$) strongly enhances the room temperature ionic conductivity of solvent-free PEO-based polymer electrolytes.[12] Lithium metal batteries based on $P(EO)_{20}LiTFSI-PYR_{13}TFSI$ ($LiTFSI = LiN(SO_2CF_3)_2$) polymer electrolyte have excellent performance at temperatures as low as 40 °C.[13] Also, the long-term viability of ionic liquids as electrolytes for supercapacitors has been demonstrated.[14] The interest in rechargeable lithium batteries and supercapacitors arises from their potential applicability for portable electronic, telecommunication, and electric vehicle propulsion technologies. The use of RTILs as replacements for solvents in electrolyte mixtures is now under investigation worldwide. Although ionic liquids consist solely of ions, these ions are not electroactive in lithium batteries, thus requiring the addition to the RTIL of a suitable lithium salt.[9,10,13,14] In a previous work, we have investigated the phase behavior of RTIL−lithium salt $(1 - x)\ PYR_{13}TFSI-(x)\ LiTFSI$ mixtures.[15] It was found that at least two crystalline complexes form with $PYR_{13}TFSI/LiTFSI$ molar ratios of 2/1 ($x = 0.33$) and 1/2 ($x = 0.67$). A eutectic also is present at a molar ratio close to $x = 0.15$. The ionic conductivity of pure $PYR_{13}TFSI$ and its mixtures with LiTFSI has also been investigated.[16] Here we report a preliminary Raman investigation of $PYR_{13}TFSI$ and a sample close to the 2/1 mixed-salt crystalline complex ($x = 0.35$) composition.

* To whom correspondence should be addressed. E-mail: passerini@casaccia.enea.it.

[†] University of Calabria.

[‡] IDROCOMB.

Experimental Section

$PYR_{13}TFSI$ was synthesized from 1-methylpyrrolidine (97%), 1-iodopropane (99%) (purchased from Aldrich and used as received), and LiTFSI (3M).[15] $PYR_{13}TFSI$ was prepared by combining 1-methylpyrrolidine with a stoichiometric amount of 1-iodopropane in ethyl acetate. The resulting crystalline $PYR_{13}I$ salt was recrystallized using acetone/ethyl acetate and washed repeatedly with ethyl acetate until a pure white salt was obtained. $PYR_{13}I$ was then dissolved in deionized water, resulting in a clear, colorless solution. A stoichiometric amount of LiTFSI dissolved in deionized water was added, and the mixture was stirred. The $PYR_{13}TFSI$ phase separated from this mixture. The aqueous phase with dissolved LiI was removed, and the remaining $PYR_{13}TFSI$ oily liquid was purified by washing repeatedly with hot deionized water. The $PYR_{13}TFSI$ was dried under high vacuum at 100 °C for 24 h and then 120 °C for 6 h. After purification and drying, the salt was a clear, colorless liquid at room temperature ($T_m = 12$ °C). The material was stored and handled in a dry room (<0.2% RH, 20 °C).

LiTFSI was dried under vacuum for 48 h at 150 °C. The $(1 - x)\ PYR_{13}TFSI-(x)$ LiTFSI ($x = 0.35$) sample was prepared by combining the two salts and heating/stirring on a hot plate until a homogeneous clear solution formed (the 2/1 complex has a $T_m = 25$ °C). The $x = 0.35$ sample crystallizes when stored in a refrigerator. The cells for the Raman experiments were prepared by sandwiching the samples between a steel substrate and thin (150 μm) glass cover slide with the edges sealed with epoxy.

Raman spectra were recorded with a software-controlled Jobin-Yvon micro-Raman LABRAM apparatus. A 17 mW He−Ne laser with a 50× Olympus focal lens was used. The spectral resolution using a grating with 1800 grooves/mm combined with the CCD detector was on the order of 1 cm^{-1}. The temperature of the samples was controlled by placing the sealed cells in a LINKAM THMS cell. To facilitate the crystallization of the samples, the cells were initially annealed to 40 °C and then slowly cooled to −100 °C at a cooling rate of 1 °C/min. The measurements were performed from low to high temperatures using a heating rate of 1 °C/min. Prior to the measurements

10.1021/jp046030w CCC: $30.25
Published on Web 12/17/2004

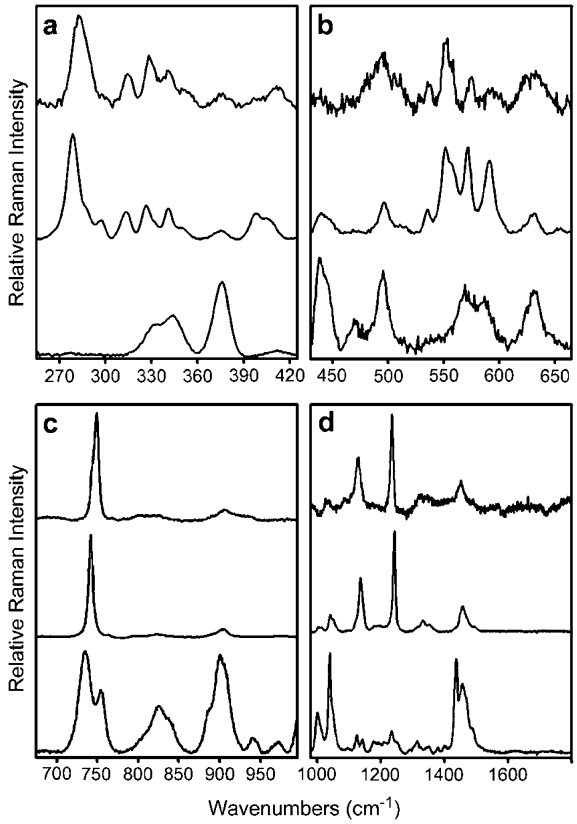

Figure 1. Raman spectra of (bottom) $PYR_{13}I$, (middle) $PYR_{13}TFSI$, and (top) $(1 - x)$ $PYR_{13}TFSI-(x)$ LiTFSI ($x = 0.35$) (the scaling of the spectra has been changed to facilitate comparisons).

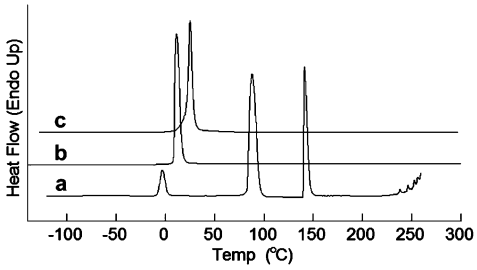

Figure 2. DSC heating traces of (a) $PYR_{13}I$, (b) $PYR_{13}TFSI$, and (c) $(1 - x)$ $PYR_{13}TFSI-(x)$ LiTFSI ($x = 0.35$).

being performed, the samples were held at the selected temperature for 40 min for thermal stabilization.

Results and Discussion

The room temperature Raman spectra of $PYR_{13}I$, $PYR_{13}TFSI$, and a $(1 - x)$ $PYR_{13}TFSI-(x)$ LiTFSI ($x = 0.35$) mixture are presented in Figure 1. At this temperature, $PYR_{13}I$ may be a plastic crystalline salt since the salt displays an endothermic peak in the DSC heating trace at -3 °C which may correspond to the onset of the rotational motion of some or all of the cations (Figure 2). $PYR_{13}TFSI$ has a melting temperature of 12 °C (Figure 2).[15] Both the $PYR_{13}I$ and $x = 0.35$ mixed salt samples are solids at room temperature, whereas $PYR_{13}TFSI$ is a liquid. The crystal structures for $PYR_{13}I$, $PYR_{13}TFSI$, and the 2/1 $PYR_{13}TFSI$/LiTFSI phase are not yet known. Note that it is possible that more than one independent PYR_{13}^+ cation conformation exists in the crystalline state, which would increase the number of observed Raman bands. Additionally, disordering of the cations (in the crystalline state or liquid phase) also complicates the band structure as the bandwidths increase due to variations in the cation conformations.

The spectrum of the ionic liquid ($PYR_{13}TFSI$) differs substantially from that of its precursor salt ($PYR_{13}I$). Although to a lesser extent, differences are also seen in the comparison of the ionic liquid and its mixture with LiTFSI. The overall intensity of the features of the $PYR_{13}TFSI$ spectrum is higher as evidenced by the higher noise present in the spectra of the solid $PYR_{13}I$ and $PYR_{13}TFSI-$LiTFSI mixture. This is obviously due to the fact that the former material is the only one fully liquid at room temperature.

The spectra of the three samples are quite complex and rich in bands. However, the comparison of the $PYR_{13}I$ spectrum with the others permits the discrimination between the bands ascribed primarily to the internal vibrational modes of the $TFSI^-$ anion and those of the PYR_{13}^+ cation. Due to the high mass of both the PYR_{13}^+ cation and I^- anion, the lattice modes of the iodide salt occur at very low frequencies, well inside the spectral region (below 200 cm^{-1}) inhibited by the notch filter of the Raman apparatus. The observed peaks and tentative peak assignments for the $TFSI^-$ anion bands are summarized in Table 1. The assignment of the $TFSI^-$ anion vibrational modes is aided by the extensive investigations performed by several research groups.[17−19]

The remaining peaks in the $PYR_{13}TFSI$ spectrum not attributed to the $TFSI^-$ anion are due to the vibrational modes of the PYR_{13}^+ cation. Some of these modes are hidden by the more intense $TFSI^-$ anion modes in $PYR_{13}TFSI$, but a comparison with the Raman spectrum of $PYR_{13}I$ enables the identification of these cation internal modes. In Figure 1a the band at 375 cm^{-1} is observed in both spectra ($PYR_{13}TFSI$, $PYR_{13}I$), while the other two bands (331 and 344 cm^{-1}) are observable only in $PYR_{13}I$ due to the intense $TFSI^-$ anion modes occurring between 300 and 350 cm^{-1}. Similarly, in Figure 1b the bands at 440 (composed of two overlapping bands at 438 and 445 cm^{-1}), 468, 495, and 631 cm^{-1} are detected in both spectra while the bands at 569 and 587 cm^{-1} are hidden by the $TFSI^-$ anion bands at 572 and 591 cm^{-1}. In Figure 1c the two bands at 735 and 754 cm^{-1} in $PYR_{13}I$ are totally hidden by the strongest $TFSI^-$ anion band occurring at 742 cm^{-1} in $PYR_{13}TFSI$. The remaining bands of the PYR_{13}^+ cation at 824, 837, 889, and 900 cm^{-1} are observed in both the $PYR_{13}I$ and $PYR_{13}TFSI$ salts. The most intense bands in $PYR_{13}I$ (1002 and 1041 cm^{-1} and the group between 1400 and 1489 cm^{-1}) are also seen in $PYR_{13}TFSI$, taking into account that mode splittings in the solid salt $PYR_{13}I$ disappear in the more symmetric liquid $PYR_{13}TFSI$.

The assignment of the vibrational modes for the PYR_{13}^+ cation is difficult since no calculations are available. The investigation of the vibrational modes and some experimental spectra have been reported for the *N*,*N*-dimethylpyrrolidinium iodide salt,[20] pyrrolidine molecule [C_4H_9N] and its derivatives,[21,22] and the bis(pyrrolidinium) chloride hexachloroantimonate(V) [$(C_4H_8NH_2^+)_2Cl^-SbCl_6^-$] mixed salt.[23] Although the cation of the dimethylpyrrolidinium iodide salt (PYR_{11}^+) is chemically similar to the PYR_{13}^+ cation, its symmetry is quite different. This difference strongly influences the Raman modes and does not allow the extension of the assignments made for PYR_{11}^+ to the PYR_{13}^+ cation.

The addition of LiTFSI to the ionic liquid causes a relative increase in the intensities of all of the modes associated with the $TFSI^-$ anion relative to the PYR_{13}^+ cation. This is to be expected given the larger fraction of $TFSI^-$ anions present in the material. In Figure 1c the most intense band of the anion appears at 742 cm^{-1}. This band was attributed to the CF_3 bending in the SCF_3 group;[24] however, in a following work it was considered as predominantly associated with the S−N

TABLE 1: Raman Modes and Relative Intensities of $PYR_{13}TFSI$ and $PYR_{13}I$[a]

$PYR_{13}TFSI$			$PYR_{13}I$	
Raman shift (cm^{-1})	relative intensity	assignment	Raman shift (cm^{-1})	relative intensity
279	S	$\rho(CF_3)$ (17)	334	MS
289	VW		344	MS
297	W		376	S
313	M	$\rho(SO_2)$ (17)	411	VW
327	M	$\rho(SO_2)$ (17)	438	MS
341	M	$\tau(SO_2)$ (17)	445	M
350	VW	$\tau(SO_2)$ (17)	469	VW
375	S		495	W
399	M	$\omega(SO_2)$ (17)	569	VW
405	M	$\omega(SO_2)$ (17)	587	VW
440	W		631	W
447	VW		735	MS
468	W		754	M
496	M		824	M
511	VW		837	M
516	VW		889	MW
535	M		900	MS
551	M	$\delta_s(SO_2)$ (17)	941	VW
556	M		972	VW
572	M	$\delta_a(CF_3)$ (17)	1002	M
591	M	$\delta_a(SO_2)$ (17)	1041	MS
632	M		1097	VW
655	VW		1125	W
742	VS	$\delta_s(CF_3)$, υ_s(SNS) (24, 25)	1144	W
764	VW	υ_s(SNS) (17)	1178	VW
797	M		1193	VW
823	M		1211	VW
906	M		1234	W
940	W		1254	VW
974	W		1316	W
1005	M		1352	VW
1014	M		1378	VW
1042	MS		1402	VW
1052	M		1438	S
1137	S	$\upsilon_s(SO_2)$ (17)	1457	MS
1182.	W		1489	MS
1192	W	$\upsilon_a(CF_3)$ (17)		
1244	S	$\upsilon_s(CF_3)$ (17)		
1317	W			
1334	M	$\upsilon_a(SO_2)$ (17)		
1354	W			
1435	VW			
1449	MS			
1459	MS			
1496	W			

[a] S = strong, MS = medium strong, M = medium, W = weak, VW = very weak. References for peak assignments are indicated in parentheses.

stretching.[25] Rey et al.[17] noted that, in fact, it involves a complex mixing of internal coordinates corresponding to the expansion and contraction of the entire $TFSI^-$ anion. This vibration induces a great change of the polarizability, and its energy is strongly affected by the coordination of the anion. In PEO−LiTFSI mixtures, for example, the band maximum is at 740 cm^{-1} and is associated with "free" (uncoordinated) $TFSI^-$ anions, while a shoulder at 746 cm^{-1} is associated with contact ion pairs ($Li^+\cdots TFSI^-$).[17−19] The band for the ionic liquid $PYR_{13}TFSI$ is well fitted by a single Lorentzian curve centered at 742 cm^{-1} (Figure 3a), whereas two Lorentzian curves are needed to fit the band of the $x = 0.35$ mixture (Figure 3b). These latter two bands are shifted toward the higher frequencies of 744 and 749 cm^{-1}. From the literature cited above, these increases in frequency of this band are due to the coordination of the $TFSI^-$ anions with Li^+ cations. In the $x = 0.35$ mixture, there are three $TFSI^-$ anions per Li^+ cation, and the vibrational bands for the

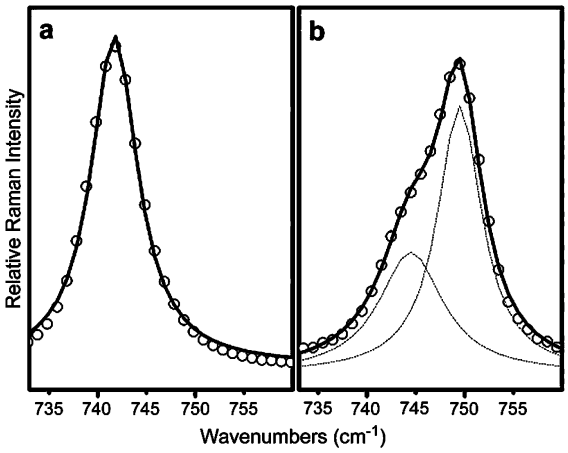

Figure 3. Raman spectra of (a) $PYR_{13}TFSI$ and (b) $(1 - x)$ $PYR_{13}TFSI-(x)$ LiTFSI ($x = 0.35$) at room temperature. The open circles are experimental data, the dashed curves are the single Lorentzian bands, and the solid line is the total fitted curve.

anion indicate that perhaps two of the anions are present as aggregates (coordinated to more than one Li^+ cation) and the third is a contact ion pair (coordinated to a single Li^+ cation) at room temperature. In addition, the observed vibrational frequency can shift depending on the prevalent conformational state of the $TFSI^-$ anion, as reported for other TFSI-based polymer electrolytes[25] and calculated for the specific case of Li−TFSI ion pairs.[26] Other bands of the $TFSI^-$ anion show a similar behavior upon the addition of LiTFSI. For example, the low-frequency band located at 280 cm^{-1}, which was also associated with the mixing of different internal modes by the theoretical investigation of Rey et al.,[17] is also seen to shift toward higher frequency in the $x = 0.35$ mixture with the concomitant appearance of a new band at a slightly higher frequency.

To evaluate the state of association of the ions in the ionic liquid and its mixture with LiTFSI, the Raman investigation was performed at several temperatures both above and below the crystallization temperature of the samples. To aid in the crystallization of the materials, the temperature was varied as follows: the temperature was increased (1 °C/min) from room temperature to 40 °C and held for about 1 h to ensure the melting of both samples. The samples were then slowly cooled (1 °C/min) to −100 °C, and the spectra were collected after the samples were held for 40 min at this temperature. The samples were then heated (1 °C/min), and the spectra were taken at 0, 20, 40, and 60 °C. The samples were held at each temperature for at least 40 min prior to collection of the Raman spectra.

The Raman spectra at different temperatures of the $PYR_{13}TFSI$ sample are shown in Figure 4. The spectra taken at low temperatures are more defined with sharper features. For instance, the most intense anion band at 742 cm^{-1} (Figure 4c) maintains its strong intensity across the solid−liquid transition, while changing its frequency (slight downshift with increasing temperature) and bandwidth (increasing the full width at half-maximum, FWHM, with increasing temperature). However, some Raman regions show substantial changes with increasing temperatures. A quite interesting effect associated with the solid−liquid transition is the disappearance of the intense peak at 299 cm^{-1} and the intensity increase of the lower frequency band at 279 cm^{-1} (Figure 4a). A possible explanation of this spectral change could involve the establishment in the solid phase of a crystal field that causes the splitting of this $TFSI^-$ internal mode ($\rho(CF_3)$). The crystal field obviously disappears when the sample melts (at 12 °C) as does the 299 cm^{-1} band.

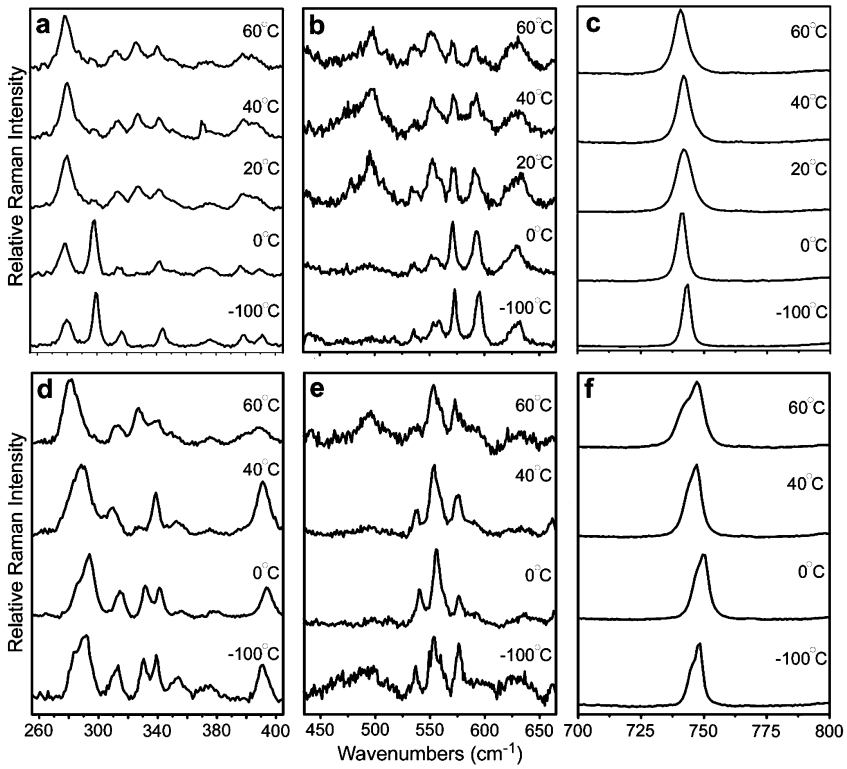

Figure 4. Selected regions of the Raman spectra of (a−c) $PYR_{13}TFSI$ and (d−f) $PYR_{13}TFSI-(x)$ LiTFSI ($x = 0.35$) collected at different temperatures (the scaling of the spectra has been changed to facilitate comparisons).

The link between the two peaks (279 and 299 cm^{-1}) is supported by the fact that the total area of the two peaks remains approximately constant. If the average molecular environment of the liquid phase is more symmetric than in the solid phase, it is also quite more disordered. As a consequence, new Raman bands arise due to the disordering-induced light scattering, i.e., random fluctuation from place to place of the molecular interactions. This effect is most likely responsible for the occurrence of broad features such as the band at about 500 cm^{-1} (Figure 4b) which is clearly visible in the liquid phase, but absent in the solid phase.

The Raman spectra at different temperatures of the $x = 0.35$ sample are also shown in Figure 4. The Raman features of the solid phase differ from those of pure $PYR_{13}TFSI$ because of the strong interaction of the Li^+ cations with the $TFSI^-$ anions. This is particularly true in the lower frequency region, where the crystalline long-range interactions can be more easily coupled to the bending internal vibration of the ions. For instance, the suggested crystal field splitting of the $\rho(CF_3)$ mode is quite small (not well separated for the two components) occurring at about 282 and 289 cm^{-1} in the $x = 0.35$ mixture compared with 279 and 299 cm^{-1} in pure $PYR_{13}TFSI$. The spectrum of Figure 4f clearly shows that the splitting and frequency increase of the most intense $TFSI^-$ band (near 740 cm^{-1}) upon LiTFSI addition to $PYR_{13}TFSI$ occurs over the entire temperature range examined. This band in the $x = 0.35$ sample is always well fitted by two Lorentzian curves, as shown in Figure 3. The relative intensity of the two components, however, changes with the melting transition and with increasing temperature in the liquid phase. When the $x = 0.35$ mixture melts, the bands located at 740−749 cm^{-1} broaden and shift to lower wavenumbers. This may reflect a weakening of the anion oxygen$\cdots Li^+$ cation coordination bonds. Additionally, one or more of the three $TFSI^-$ anions present per Li^+ cation may become uncoordinated due to thermal energy and steric effects. These effects would account for the lowering of the band wavenumber.

Conclusions

A preliminary Raman vibrational spectroscopic investigation for the room temperature ionic liquid $PYR_{13}TFSI$ and a mixture of this salt with LiTFSI is reported here. The analysis of the band structure for the pyrrolidinium cation is complicated by factors such as a lack of knowledge regarding the equivalency of the cations in the crystalline state and possible disordering of the cations in both the crystalline and melt states. Some information regarding the interactions between the $TFSI^-$ anions and $PYR_{13}{}^+$ and Li^+ cations suggests that the anions have only a very weak interaction with the organic, sterically shielded cations, but strong coordination to the Li^+ cations. Multiple forms of $Li^+\cdots TFSI^-$ ionic coordination appear to exist in the mixed salt crystalline complex, and this coordination changes somewhat in the molten state.

References and Notes

(1) Adam, D. *Nature* **2000**, *407*, 938.
(2) Earle, M. J.; Seddon, K. R. *Pure Appl. Chem.* **2000**, *72*, 1391.
(3) Anderson, J. L.; Ding, J.; Welton, T.; Armstrong, D. W. *J. Am. Chem. Soc.* **2002**, *124*, 14247.
(4) Dupont, J.; de Souza, R. F.; Suarez, P. A. Z. *Chem. Rev.* **2002**, *102*, 3667.
(5) Bhatt, A. I.; May, I.; Volkovich, V. A.; Hetherington, M. E. Lewin, B.; Thied, R. C.; Ertok, N. *J. Chem. Soc., Dalton Trans.* **2002**, 4532.
(6) Panozzo, S.; Armand, M.; Stéphan, O. *Appl. Phys. Lett.* **2002**, *80*, 679.
(7) Wang, P.; Zakeeruddin, S. M.; Exnar, I.; Grätzel, M. *Chem. Commun.* **2002**, 2972.
(8) Fuller, J.; Breda, A. C.; Carlin, R. T. *J. Electroanal. Chem.* **1998**, *459*, 29.
(9) Nakagawa, H.; Izuchi, S.; Kuwana, K.; Nukuda, T.; Aihara, Y. *J. Electrochem. Soc.* **2003**, *150*, A695.
(10) Sakaebe, H.; Matsumoto, H. *Electrochem. Commun.* **2003**, *5*, 594.

(11) Noda, A.; Susan, M. A. B. H.; Kudo, K.; Mitsushima, S.; Hayamizu, K.; Watanabe, M. *J. Phys. Chem. B* **2003**, *107*, 4024.

(12) Shin, J.-H.; Henderson, W. A.; Passerini, S. *Electrochem. Commun.* **2003**, *5*, 1016.

(13) Shin, J.-H.; Henderson, W. A.; Passerini, S. *Electrochem. Solid State Lett.*, in press.

(14) Balducci, A.; Henderson, W. A.; Mastragostino, M.; Passerini, S.; Simon, P.; Soavi, F. *Electrochim. Acta*, in press.

(15) Henderson, W. A.; Passerini, S. *Chem. Mater.* **2004**, *16*, 2881.

(16) Henderson, W. A.; Shin, J.-H.; Passerini, S. Manuscript in preparation.

(17) Rey, I.; Johansson, P.; Lindgren, J.; Lassegues, J. C.; Grondin, J.; Servant, L. *J. Phys. Chem. A* **1998**, *102*, 3249.

(18) Edman, L. *J. Phys. Chem. B* **2000**, *104*, 7254.

(19) Rey, I.; Lassegues, J. C.; Grondin, J.; Servant, L. *Electrochim. Acta* **1998**, *43*, 1505.

(20) Adebahr, J.; Johansson, P.; Jacobsson, P.; MacFarlane, D. R.; Forsyth, M. *Electrochim. Acta* **2003**, *48*, 2283.

(21) Billes, F.; Geidel, E. *Spectrochim. Acta, Part A* **1997**, *53*, 2537.

(22) El-Gogary, T. M.; Soliman, M. S. *Spectrochim. Acta, Part A* **2001**, *57*, 2647.

(23) Bednarska-Bolek, B.; Jakubas, R.; Bator, G.; Baran, J. *J. Mol. Struct.* **2002**, *614*, 151.

(24) Huang, W.; Frech, R.; Wheeler R. A. *J. Phys. Chem.* **1994**, *98*, 100.

(25) Bakker, A.; Gejji, S.; Lindgren, J.; Hermansson, K.; Probst, M. M. *Polymer* **1995**, *36*, 4371.

(26) Gejji, S.; Suresh, C. H.; Babu, K.; Gadre, S. R. *J. Phys. Chem. A* **1999**, *103*, 7474.